

COLOR DISTRIBUTION OF GALAXIES IN THE CFHTLS-DEEP FIELDS

Florence Ienna, and Roser Pelló¹

Abstract. We present the results obtained on the color distribution of galaxies in the CFHTLS-Deep Field Survey Data Release 03². Photometric redshifts have been computed using a standard SED fitting approach, with a new version of the public code HyperZ (New-HyperZ). Large samples of galaxies with well determined photometric redshifts in the $0 < z < 1.3$ interval have been selected in the four CFHTLS Deep fields, within the completeness limit in absolute luminosity in u and r bands. We study the restframe color distribution of galaxies as a function of redshift, luminosity and local density. Our results are consistent with a bimodal color distribution, where red galaxies dominate the highest luminosities out to $z \sim 0.6$. An important population of blue and bright galaxies appears beyond this redshift, increasing with redshift. Out to $z \sim 1.3$, a strong evolution is observed, at a given redshift, in the color distribution of galaxies as a function of luminosity, together with a mild evolution with the local density at fixed luminosity.

1 Introduction

Considerable progress has been made during the last ten years on the study of galaxy properties and their evolution out to redshifts $z \sim 1$, thanks to large surveys (e.g.:Canada-France Redshift Survey; Lilly et al. 1995; 2 Degree Field Survey; Colless et al. 2001). More recently, the SDSS (Sloan Digital Sky Survey; York et al. 2000) has allowed the extragalactic community to study the local universe using an extremely large sample of galaxies. Different attempts have been made to constrain the global photometric properties of galaxies up to $z \sim 6$ based on deep high-resolution imaging surveys (Hubble Deep Fields; Williams et al. 1996; Hubble Ultra Deep Field; Beckwith et al. 2006). However, these deep pencil-beam surveys based on photometric redshifts include a relatively small sample of galaxies compared to local samples. All this studies have demonstrated the existence of strong correlations between galaxy rest-frame properties, morphology and environment. Substantial progress will be provided by Large spectroscopic datasets, combined with photometric multi-band data (e.g.:Franzetti et al. (2006) using the VIMOS-VVDS data).

The combination of homogeneous wavelength coverage and photometric depth on the large effective area achieved by the CFHTLS (Canada-France-Hawaii Telescope Legacy Survey) allows the study of galaxy evolution with unprecedented accuracy and is particularly well suited for a detailed study of galaxy populations at $z \sim 0.2 - 1.3$. A recent paper by Nuijten et al. (2005) addresses the relationships between galaxy morphology, luminosity, color and environment as a function of redshifts using a sample of ~ 65000 galaxies selected in one of the CFHTLS Deep fields (hereafter CFHTLS-D). These authors find a bimodal color distribution for galaxies out to $z \sim 1$, with a prominent red sequence at $0.2 < z < 0.4$, and a large blue population at $0.8 < z < 1$.

We analyse in this paper the color distribution of galaxies out to $z \sim 1.3$, using a template fitting method to derive photometric redshifts and restframe properties for galaxies in the T0003 release of the CFHTLS-D. In Sect. 2 we describe the CFHTLS-D data used in this study. Photometric redshifts are presented in Sect. 3, together with the sample selection used in this study. Results are summarized in Sect. 4. More details will be given in a forthcoming paper (Ienna & Pelló, in preparation). We adopt the cosmological parameters $\Omega_\Lambda = 0.7$, $\Omega_m = 0.3$, and $H_0 = 70 \text{ km s}^{-1} \text{ Mpc}^{-1}$. Magnitudes are given in the AB system (Oke 1974).

¹ Laboratoire d'astrophysique de Toulouse et Tarbes, UMR 5572, Université Paul Sabatier Toulouse 3, CNRS, 14 avenue Edouard Belin, 31400 Toulouse, FRANCE.

² Based on observations obtained with MegaPrime/MegaCam, a joint project of CFHT and CEA/DAPNIA, at the Canada-France-Hawaii Telescope (CFHT), which is operated by the National Research Council (NRC) of Canada, the Institut National des Sciences de l'Univers of the Centre National de la Recherche Scientifique (CNRS) of France, and the University of Hawaii. This work is based in part on data products produced at TERAPIX and the Canadian Astronomy Data Center as part of the Canada-France-Hawaii Telescope Legacy Survey, a collaborative project of NRC and CNRS.

2 The Data

The CFHTLS covers 4 square degrees in four independent fields (D1, D2, D3, D4), observed through five bands in the visible domain: u^* , g' , r' , i' , z' . The data were processed at Terapix (astrometry, photometric calibration, image stacking, detection and photometric catalogs). More details can be found on the Terapix¹ website. In this study we used the CFHTLS T0003 release which includes observations from June 2003 to July 2005. The image quality in the final stack ranges between $0.8''$ in z' and $1.0''$ in u^* . The four catalogs released by Terapix included more than 1.6 million objects in total, up to $AB \sim 27.3$ in u^*g' , $AB \sim 27$ in $r'i'$, and $AB \sim 26$ in z' (SExtractor MAG_AUTO, 1σ detection limit).

3 Photometric redshift and sample selection

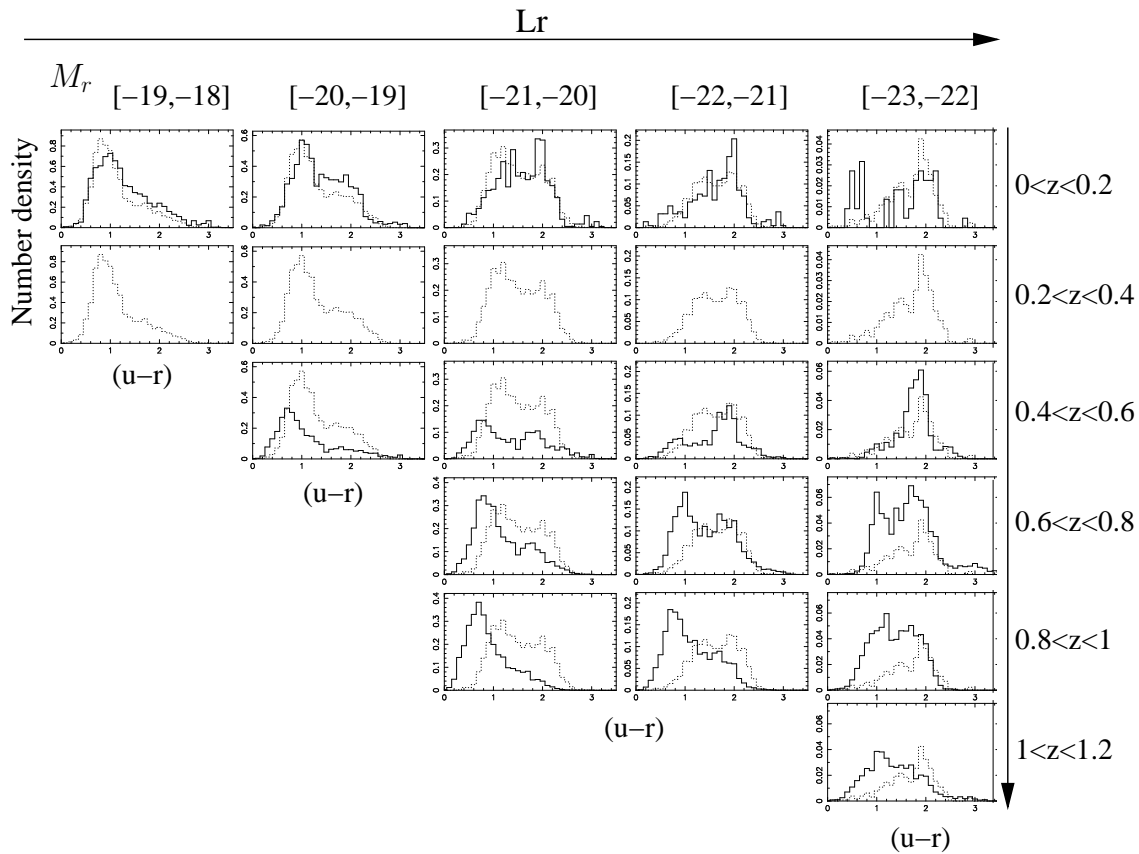


Fig. 1. Number density of galaxies (in units of 10^{-3} galaxies Mpc^{-3}) as a function color. The evolution of this relationship is presented as a function of redshift (increasing from top to bottom) and luminosity (increasing from left to right). The distribution of galaxies in the $z=0.2-0.4$ bin is superimposed to all diagrams for comparison (dashed line). The histogram at the bottom left presents the redshift distribution for different i -band selected samples. This diagram is a combination of the four CFHTLS Deep Fields.

Photometric redshifts (hereafter z_{phot}) have been computed with a new version of the public code *Hyperz* (*new-hyperz*²), originally developed by Bolzonella et al. (2000). This method is based on the fitting of the photometric Spectral Energy Distributions (SED) of sources using a large set of templates. In this case, the

¹<http://terapix.iap.fr>

²<http://www.ast.obs-mip.fr/users/roser/hyperz/>

template library includes 14 templates: 8 evolutionary synthetic SEDs computed with the last version of the Bruzual & Charlot code (Bruzual & Charlot 1993), with Chabrier (2003) IMF; 4 empirical SEDs from Coleman, Wu and Weedman (1980), and 2 starburst galaxies from Kinney et al. (1996). Internal extinction is considered as a free parameter following the Calzetti's (2000) law, with $E(B-V) \sim 0.45$ mags. Galactic extinction is also corrected. Photometric redshifts were computed in the range $z=0-6$. No luminosity prior was used, but a simple cut in the permitted range of luminosities: $M_B = [-14, -23]$. SExtractor MAG_AUTO magnitudes and errors were used to compute z_{phot} . When an object is non-detected in a given filter, the flux in this filter is set to 0, with an error bar corresponding to a $S/N \sim 1$ in this filter. We have also corrected for seeing differences between the different images, taking the i-band image as a reference. The photometric redshift accuracy was estimated by a direct comparison with secure spectroscopic samples available in the Groth/Deep Survey (D3) (see more details in our web page³). Similar results are obtained using the VVDS spectroscopic sample (D1, Ilbert et al. 2006). Due to the lack of near-IR filters, we expect to obtain accurate z_{phot} for our sample up to $z \sim 1.3$. A blind comparison with spectroscopic redshifts yields a mean dispersion $\sigma(\Delta z / (1+z)) = 0.056$ for the whole sample within $z = 0 - 1.3$. All objects in masks, saturated sources and bright stars up to $i < 22$ have been removed from the sample. Only sources detected in at least two different filters with $S/N \geq 3$ have been considered. An additional selection has been introduced based on the quality of the fit, affecting only $\sim 10\%$ of the remaining objects. The final sample used in this study contains 1.13 million sources over 4 square degrees.

4 Results: Color distribution out to $z=1.3$

In order to address the evolution of the color distribution of galaxies as a function of redshift and local density, we have defined samples of sources which are complete in *all* the filters considered simultaneously (here the restframe u^* and r' bands). Different samples are selected here in absolute magnitude M_r as a function of redshift, in such a way that for galaxies brighter than M_r , the limiting M_u allows to reach at least a restframe $u - r \leq 3.5$. The limiting magnitudes in this complete sample of ~ 0.9 million galaxies are $M_r \leq -18$ for $z \leq 0.4$, $M_r \leq -19$ for $z \leq 0.6$, $M_r \leq -20$ for $z \leq 1.0$, and $M_r \leq -22$ for $z \leq 1.2$. The evolution of the restframe color $u - r$ as a function of redshift and luminosity is presented in Fig. 1. A bimodal color distribution is observed at all redshifts and luminosities. From recent studies of the local universe (e.g. Balogh et al. 2004, Hogg et al. 2003, Cooper et al. 2006), it is admitted that this bimodal distribution corresponds to a separation between red early type galaxies (ellipticals with old stellar passively evolving population) and blue late type galaxies (spirals with a young stellar population). The color distribution shown in Fig. 1 is bimodal out to $z \sim 1.2$. The red population is found to dominate the brightest luminosity bins out to $z \sim 0.6$. Its mean color becomes bluer with increasing redshift. Although a red and bright population still exists at $z \sim 1.2$, the blue population dominates at $z \sim 0.8-1.2$ in all the luminosity bins. The blue population also dominates in the lowest luminosity bins at low redshift, and becomes more important with increasing redshift. Also the mean color of this population becomes bluer with increasing redshift. Our results at $z \leq 0.4$ are in good agreement with those found in the local universe (e.g. Baldry et al. 2004), although our sample is much less significant in the brightest bin at $z \leq 0.2$.

We have studied the relationship between color distribution and environment taking advantage of the large complete sample of galaxies in the CFHTLS-D. A local density estimator has been derived for each object based on the distance to the 10th closest neighbour D : $\Sigma_{10} = 10 / (\pi * D^2)$, where D is the projected linear distance at z_{phot} . Close neighbours are selected within a photometric redshift slice $z_{phot} \pm 0.1$, with M_r in the $[-24, -20]$ interval. This is the z_{phot} equivalent of the estimator used by Balogh et al. (2004) with the SDSS spectroscopic sample. Fig. 2 displays the number density of galaxies as a function color, for three representative redshift bins, and for five density regimes (roughly the same used by Balogh et al. (2004) in the SDSS). At redshift between $0 < z < 0.6$ we observe the same trends as in the SDSS. The blue population dominates the lowest density and faintest luminosity bins, whereas the red population is found to dominate the highest density and brightest luminosity bins. These general trends seem more sensitive to the luminosity than to the local density. At $z > 0.8$, a bright blue population appears even in the densest regions, increasing with redshift.

In conclusion, the optimal combination of homogeneous wavelength coverage and photometric depth on the large effective area achieved by the CFHTLS-D T0003 allows the study of photometrical properties of galaxies with unprecedented accuracy.

³<http://www.ast.obs-mip.fr/users/rosier/CFHTLS-T0003/>

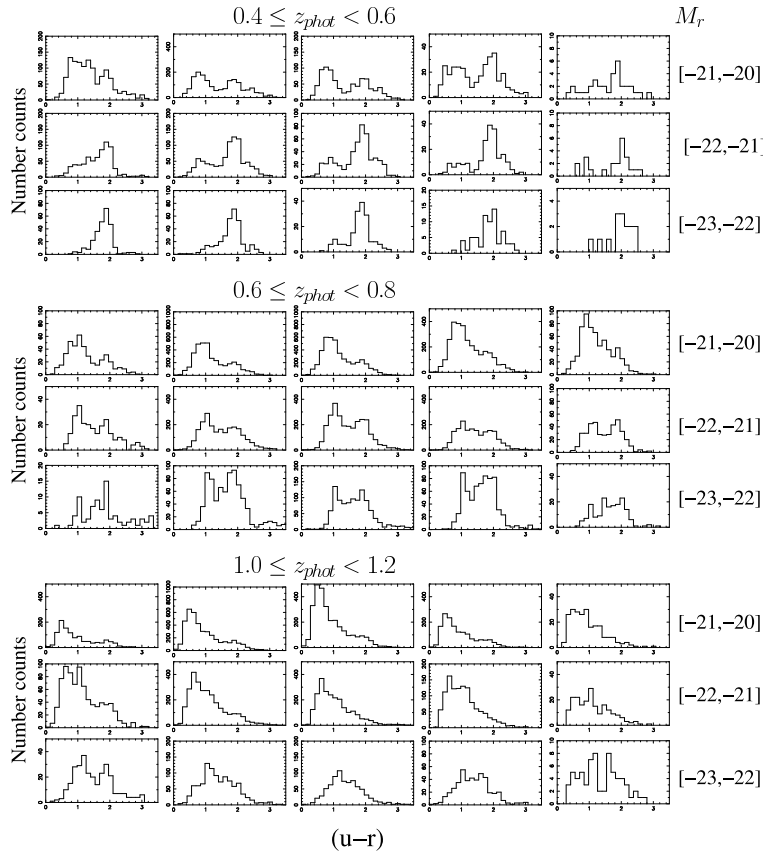


Fig. 2. Number density of galaxies (in units of 10^3 galaxies Gpc^{-3}) as a function color. The evolution of this relationship is presented as a function of the local density (increasing from left to right) and luminosity, for three representative redshifts.

References

- Balogh, M. L., Baldry, I.K., Nichol, R., Miller, C., Bower, R. and Glazebrook, K. 2004, *ApJ*, 615, L101
 Baldry, I.K., Balogh, M. L., Bower, R., Glazebrook, K. and Nichol, R. 2004, *AIP Conf. Proc.*, 743(2004) 100-119
 Beckwith, S. V. W., et al. 2006, *AJ*, 132, 1729
 Bolzonella, M., Miralles, J. M., & Pello, R., 2000, *A&A*, 363, 476-492
 Chabrier, G. 2003, *PASP*, 115, 763
 Coe, D., Benítez, N., Sánchez, S. F., Jee, M., Bouwens, R., & Ford, H. 2006, *AJ*, 132, 926
 Coleman, G. D., Wu, C.-C., & Weedman, D. W. 1980, *ApJ*, 43, 393
 Colless, M.M., et al. 2001, *MNRAS*, 328, 1039
 Cooper, M. C., et al. 2006, *MNRAS*, accepted [astro-ph/0603177]
 Croton, D. J., et al. 2005, *MNRAS*, 356, 1155
 Dressler, A. 1980, *ApJ*, 236, 351
 Franzetti, P, et al. 2006, submitted to *A&A*, astro-ph/0607075.
 Hogg, D. W., et al. 2003, *ApJ*, 585, L5
 Ilbert, O., et al. 2006, *A&A*, 457, 841
 Kinney et al. 1996
 Kennicutt, R. C., Jr. 1983, *AJ*, 88, 483
 Lilly, S. J., Le fèvre, O., Crampton, D., Hammer, F., & Tresse, L. 1995, *ApJ*, 455, 50
 Nuijten, M. J. H. M., Simard, L., Gwyn, S., Rottgering, H. J. A. 2005, *ApJ*, 626, L77

- Wiegert, T., de Mello, D. F., & Horellou, C. 2004, *A&A*, 426, 455
Williams, R. E., et al. 1996, *AJ*, 112, 1335
Withmore, B. C., Gilmore, D. M., & Jones, C. 1993, *ApJ*, 407, 489
York, D. G., Adelman, J., Anderson, J. E. et al. 2000, *AJ*, 120, 1579